ELSEVIER

Journal of Fluids and Structures 25 (2009) 731–741

JOURNAL OF FLUIDS AND STRUCTURES

www.elsevier.com/locate/jfs

Vortex-induced vibration of two circular cylinders at low Reynolds number

T.K. Prasanth, Sanjay Mittal*

Department of Aerospace Engineering, Indian Institute of Technology, Kanpur, UP 208 016, India

Received 27 April 2008; accepted 11 December 2008
Available online 10 February 2009

Abstract

Vortex-induced vibration of a pair of equal-sized circular cylinders in tandem and staggered arrangements in laminar flow regime is investigated. A stabilized finite element method is utilized to carry out the computations in two dimensions. Both cylinders are free to oscillate in transverse as well as in-line directions. The Reynolds number, based on the free-stream speed, U, and the diameter, D, of the cylinders is 100. To encourage high amplitude of oscillation the structural damping is set to zero and cylinders of low nondimensional mass are considered ($m^* = 10$). The computations are carried out for various values of reduced speed of the oscillator ($2 \leqslant U^* \leqslant 15$). The cylinders are separated by $5.5D$ in the streamwise direction. They are separated by $0.7D$ in the cross-flow direction to study the effect of stagger. The downstream cylinder lies in the wake of the upstream one and experiences an unsteady inflow. The upstream cylinder in both tandem and staggered arrangement responds qualitatively similarly to a single cylinder. Compared to an isolated cylinder, a small increase in transverse oscillation amplitude of the upstream cylinder is observed due to the presence of the downstream cylinder. In both arrangements, the downstream cylinder shows very large amplitude transverse oscillations comparable to that of a single cylinder at higher Re. In the staggered arrangement, very large streamwise oscillations of the downstream cylinder are observed. Compared to an isolated cylinder, the synchronization range for the two-cylinder arrangement is larger. The downstream cylinder in the staggered arrangement undergoes two types of motion: an orbital motion at most of the U^* studied, and figure-of-eight motion for a small range of U^*. In the tandem arrangement, only the figure-of-eight motion is observed. The stagger in the arrangement of the two cylinders is found to have a significant effect on the flow.

Keywords: Two cylinders; Tandem and staggered; Vibration; Flow-induced; Vortex shedding

1. Introduction

Vortex-induced vibration involving more than one bluff body is an extremely complex flow problem. It is encountered in many practical situations such as flow past heat exchanger tubes, riser tubes and multiple chimney stacks to name a few. The vortex-induced vibration of a single cylinder has been studied extensively. Comprehensive reviews of the same can be found in Bearman (1984), Williamson and Govardhan (2004) and Sarpkaya (2004). A phenomenon associated with free vibrations of a cylinder is synchronization/lock-in. For a certain range of reduced

*Corresponding author. Tel.: +91 512 259 7906; fax: +91 512 259 7561.
E-mail address: smittal@iitk.ac.in (S. Mittal).

0889-9746/$ - see front matter © 2008 Elsevier Ltd. All rights reserved.
doi:10.1016/j.jfluidstructs.2008.12.002

speed the vortex shedding frequency is identical to the cylinder vibration frequency. The reduced speed, U^*, is defined as $U/f_N D$ where, U is the free-stream speed, f_N is the natural structural frequency of the oscillator and D is the diameter of the cylinder. Khalak and Williamson (1999) showed that depending on the combined mass-damping parameter, $m^*\zeta$, two types of responses are possible in the moderate Re regime ($5000 \leqslant \mathrm{Re} \leqslant 16\,000$). For low $m^*\zeta$ the response consists of three branches: initial, upper and lower. These branches are also associated with different modes of vortex-shedding and amplitudes of oscillation. For high $m^*\zeta$, only two response branches are seen. Synchronization/lock-in is observed in the laminar regime also. Even for very low $m^*\zeta$, only two branches are observed in the laminar regime. The maximum amplitude of oscillation is $\sim 0.55D$ compared to $\sim 1.1D$ at higher Re (Singh and Mittal, 2005; Prasanth and Mittal, 2008).

Most of the studies involving multiple cylinders are based on experimental investigations. Zdravkovich (1977) classified the arrangement of two stationary cylinders into three categories based on their spacing and orientation to the flow direction. Proximity interference takes place when the cylinders are placed very close to each other. Wake interference occurs when the downstream cylinder is partly or fully submerged in the wake of the upstream cylinder. Both, proximity and wake interference are encountered in the overlapping regime. Mittal et al. (1997), in their numerical study for a pair of cylinders in tandem and staggered arrangements at $\mathrm{Re} = 100$ and 1000, observed that the downstream cylinder lying in the wake of upstream one experiences large unsteady forces. Compared to the tandem arrangement, the staggered arrangement leads to higher unsteady drag force on the downstream cylinder. However, the unsteady lift force experienced by the downstream cylinder is comparable in both arrangements for stationary cylinders. Sumner et al. (2000) reported different flow patterns possible for flow past two stationary cylinders in staggered arrangement.

Very few systematic studies to understand vortex-induced vibration problems involving two cylinders have been undertaken in the past (Zdravkovich, 1985; Bokaian and Geoola, 1984; King and Johns, 1976; Laneville and Brika, 1999). When the cylinders are well separated, the downstream cylinder undergoes wake-induced galloping (Assi et al., 2006; Jester and Kallinderis, 2004). Mahir and Rockwell (1996) have shown that two cylinders subjected to forced oscillation can generate locked-in patterns of vortices over a range of excitation frequencies. Mittal and Kumar (2001) in their study of free vibrations of two equal-sized cylinders reported wake-induced flutter for the downstream cylinder. Their study was carried out for both tandem and staggered arrangements of the two cylinders at $\mathrm{Re} = 100$ for three values of nondimensional structural frequency that were either close to or equal to the vortex-shedding frequency for the stationary cylinders. The upstream cylinder was found to behave like a single cylinder. The cylinders were separated by a distance of $5.5D$ in the streamwise direction. A similar study was conducted later at $\mathrm{Re} = 1000$ (Mittal and Kumar, 2004).

In this study, computational results are presented for the vortex-induced vibration of two equal-sized cylinders in tandem and staggered arrangement at $\mathrm{Re} = 100$. The reduced speed is varied from 2 to 15. The main objective of the present work is to study the effect of stagger in free vibration of two equal-sized cylinders at low Re. To this extent, free vibrations of two cylinders separated by $5.5D$ in the streamwise direction is studied. In the first case, the cylinders are in tandem. In the second case, they are staggered by $0.7D$ in the cross-flow direction.

The outline of the rest of the article is as follows: a brief description of the governing equations and finite element formulation are given in Sections 2 and 3, respectively. The problem set-up is defined along with the boundary conditions and mesh moving scheme in Section 4. Results are presented in Section 5 and we end with a few concluding remarks in Section 6.

2. The governing equations

The flow is modelled by the Navier–Stokes equations in two dimensions in terms of primitive variables: the velocity, $\mathbf{u}$, and pressure, p. The flow is assumed to be incompressible. The motion of the body, in the two directions along the Cartesian axes, is governed by the following equations:

$$\ddot{X} + 4\pi F_N \zeta \dot{X} + (2\pi F_N)^2 X = \frac{2C_D}{\pi m^*} \quad \text{for } (0, T), \tag{1}$$

$$\ddot{Y} + 4\pi F_N \zeta \dot{Y} + (2\pi F_N)^2 Y = \frac{2C_L}{\pi m^*} \quad \text{for } (0, T). \tag{2}$$

Here, F_N is the reduced natural frequency of the oscillator. It is defined as $f_N D/U$ where f_N is the natural frequency of the oscillator in vacuum. Another related parameter is the reduced velocity, U^*. It is defined as $U^* = U/f_N D = 1/F_N$. ζ is the structural damping ratio and m^* the nondimensional mass of the body. It is defined as $m^* = 4m/(\pi\rho D^2)$ where m is the mass of the oscillator per unit length and ρ the density of the fluid. C_L and C_D are the instantaneous lift and drag

coefficients for the body, respectively. They are computed by carrying out an integration that involves the pressure and viscous stresses, around the circumference of the cylinder. The free-stream flow is assumed to be along the x-axis. $\ddot{X}$, $\dot{X}$ and X denote the normalized in-line acceleration, velocity and displacement of the body, respectively, while $\ddot{Y}$, $\dot{Y}$ and Y represent the same quantities associated with the cross-flow motion. In the present study, in which the rigid body is a circular cylinder, the displacement and velocity are normalized by the diameter, D, of the cylinder and the free-stream speed, U, respectively.

3. Finite element formulation

To accommodate the motion of the cylinders and the deformation of the mesh, the deforming spatial domain/stabilized space-time (DSD/SST) method (Tezduyar et al., 1992a, b) is utilized. The basis functions used to approximate the pressure and velocity are bilinear in space and linear in time. Details on the formulation including those on the stabilization coefficients and its implementation for oscillating cylinders can be found in articles by Tezduyar et al. (1992a–c), Singh and Mittal (2005) and Prasanth and Mittal (2008).

4. Problem description

Two cylinders, each of diameter, D, and nondimensional mass, $m^* = 10$, are mounted on elastic supports. The cylinders are free to vibrate in both streamwise and transverse directions. The nondimensional distance between the centres of the two cylinders is denoted by P/D in the streamwise direction and T/D in the cross-flow direction as shown in Fig. 1. Computations have been carried out for cylinders in tandem and staggered arrangements. In both cases, P/D is 5.5. For the staggered arrangement, T/D is 0.7. With this arrangement the downstream cylinder is expected to lie in the unsteady wake of the upstream one. To encourage high amplitude oscillations the structural damping coefficient is set to zero. The springs in both the streamwise and transverse directions are assumed to be linear and have the same stiffness. The Reynolds number is 100 and the reduced velocity, U^*, is varied from 2 to 15.

Blockage has a very significant effect on the response of cylinder undergoing vortex-induced vibrations (Prasanth et al., 2006; Prasanth and Mittal, 2008). In particular, for $m^* = 10$ and Re$\sim$100 it was shown by Prasanth and Mittal (2008) that a blockage of more than 2.5% can lead to hysteresis in the flow and response of the cylinder at the onset of synchronization. Compared to an unbounded flow, higher blockage also leads to error in the prediction of aerodynamic forces. In the present study, the lateral boundaries are located at $25D$ each from the upstream cylinder centre. The resulting blockage is 2%. The upstream and downstream boundaries are placed at $25D$ and $105.5D$ from the centre of the upstream cylinder, respectively.

4.1. Boundary conditions

The no-slip condition is applied on the velocity at the surface of the two cylinders. The flow velocity of each of the two cylinders and their locations are updated at each nonlinear iteration by solving the equations of motion for each oscillator. The outer boundary of the computational domain is a rectangle. Free-stream values are assigned to the velocity at the upstream boundary and the viscous stress vector is set to zero at the downstream boundary. On the upper

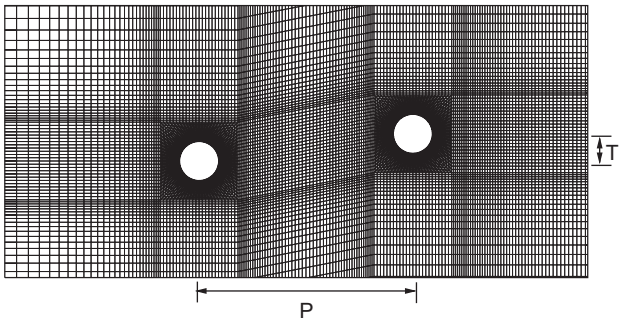

Fig. 1. A close-up view of the finite element mesh for the cylinders in staggered arrangement.

and lower boundaries, the normal component of the velocity and the component of the stress vector along the boundaries are prescribed zero values.

4.2. Finite element mesh and mesh moving scheme

A close-up view of the finite element mesh used for the computation is shown in Fig. 1. The mesh consists of 40 197 nodes and 39 648 quadrilateral elements. A more refined mesh with 80 085 nodes and 79 272 elements was used to study the spatial resolution. For the two cylinders in tandem arrangement and $U^* = 5.5$ the results from the two meshes were found to be in very good agreement. Amongst all the quantities the maximum deviation was observed for the maximum value of lift coefficient. It was 2% for the upstream cylinder and 3% for the downstream one. This establishes the adequacy of the mesh used in the present study. Each cylinder resides in a square box. The mesh moving scheme has been designed such that the mesh in the square box around each of the two cylinders moves along with it as a rigid body. The location of the outer boundary is fixed. As a result, the movement of the cylinder causes deformation of the mesh points lying between the two squares and the outer boundary. This kind of mesh movement is very inexpensive, retains the connectivity of the nodes and is expected to lead to almost no projection errors in the near wake of the cylinders.

5. Results

5.1. Transverse response

The effect of stagger in the arrangement of the two cylinders on free vibration is studied. The response of the cylinders in tandem and staggered arrangements are compared to each other and with that of an isolated cylinder. Singh and Mittal (2005) carried out a detailed study for free vibration of a single cylinder at $\mathrm{Re} = 100$. The results from that study are used here for comparison. Fig. 2 shows the variation of maximum transverse oscillation amplitude with U^* of cylinders in both arrangements. From Fig. 2(a) it is seen that the behaviour of upstream cylinder is very similar to that of a single cylinder. The upstream cylinder undergoes synchronization for $4.1 < U^* < 8.3$. The peak amplitude of the cylinder response occurs at the same U^* for upstream and single cylinders. However, the peak amplitude of oscillation observed for the upstream cylinder is slightly larger than that for the single cylinder.

The transverse response of the downstream cylinder is very different from the upstream one. The peak amplitude of oscillation observed is $\sim 1.1D$ for the downstream cylinder while it is $\sim 0.6D$ for the upstream one. Interestingly, this value is the same as that observed for free vibration in the higher Re regime (Khalak and Williamson, 1999) for cylinders with low $m^*\zeta$. Despite the similarity in maximum oscillation amplitude, the free vibrations of a single cylinder at higher Re exhibits differences with respect to the free vibrations of the downstream cylinder in the laminar regime. For example, the response of the cylinder in the laminar regime is associated with only two branches: initial and lower. On the other hand, at higher Re, an additional upper branch is observed (Khalak and Williamson, 1999).

Some other differences between the upstream and downstream cylinder are seen in Fig. 2. For the upstream cylinder, the peak amplitude of oscillation is observed near the lower U^* end of the synchronization regime. However, for the downstream cylinder it occurs near the higher U^* end of the synchronization regime. Unlike the upstream cylinder, the

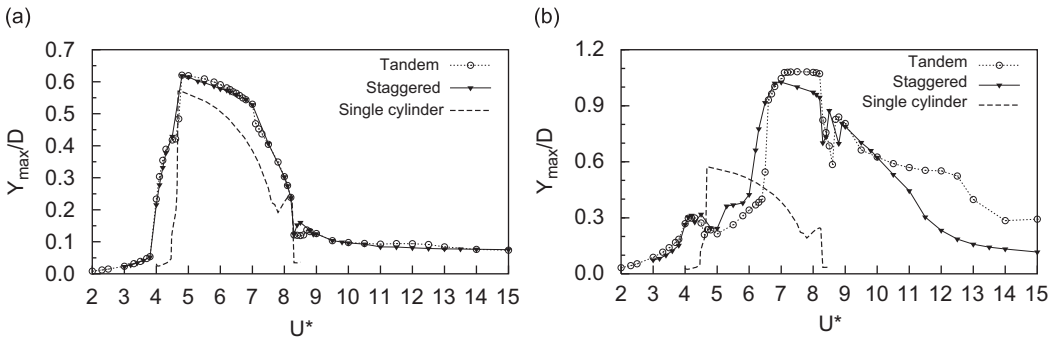

Fig. 2. Variation of the maximum transverse amplitude of oscillation of (a) upstream cylinder and (b) downstream cylinder in both tandem and staggered arrangements with U^*. The results for a single cylinder are also shown in the figure.

downstream cylinder result shows local peaks near both ends of the synchronization regime. The variation of maximum transverse amplitude with U^* of the downstream cylinder in both tandem and staggered arrangements are found to be very similar. However, the time histories of the response are quite different. As will be seen later in the paper, the stagger in the arrangement leads to variation in the vortex dynamics of the flow structures originating from the upstream cylinder and interacting with the downstream one.

5.2. *x-y trajectory of cylinders*

In general, the trajectory of a single cylinder undergoing vortex-induced vibration resembles a "figure of 8". This is because the dominant frequency in the variation of drag is twice that for the lift. In the case of two cylinders the upstream one exhibits a similar behaviour. Fig. 3 shows the Lissajous figures for the response of the downstream cylinder in tandem (top row) and staggered (bottom row) arrangement at various U^*. The downstream cylinder in the tandem arrangement undergoes a figure of 8 motion. However, it shows a different behaviour in the staggered arrangement. An orbital motion is observed during the entire U^* range except for $7.1 < U^* < 8.3$. It is found that the time variation of both lift and drag experienced by the downstream cylinder has two dominant frequencies when it undergoes orbital motion. The most dominant frequency corresponds to the vortex shedding frequency while the second one is twice the first. The figure of 8 motion is observed for $7.1 < U^* < 8.3$. In this regime, the downstream cylinder undergoes close to peak amplitude of oscillation. Fig. 3 shows that the trajectory of downstream cylinder in the staggered arrangement exhibits considerable variation with U^*.

5.3. *In-line response*

Fig. 4 shows the variation of *rms* value of in-line oscillation for cylinders in both tandem and staggered arrangement with U^*. The response of the upstream cylinder in both arrangements is qualitatively similar to that of single cylinder. However, the peak amplitudes observed are much larger for the upstream cylinder compared to the single cylinder. Multiple local peaks are observed for the upstream cylinder at both sub- as well as super-harmonics of f_N corresponding to $U^* = 6$. The downstream cylinders show vigorous oscillations compared to upstream and an isolated single cylinder. This is also observed from the Lissajous figures shown in Fig. 3. From Figs. 2 and 4 we observe that the effect of stagger is more significant in the in-line oscillations as compared to the transverse response.

5.4. *Aerodynamic coefficients*

Fig. 5 shows the variation of the maximum lift coefficient with U^* for cylinders in both tandem and staggered arrangement. The variation of maximum lift coefficient for the upstream cylinder in both the arrangements is similar to that of a single cylinder. The variation for the downstream cylinder is however, very different. Even before the onset of synchronization $C_{L_{\max}}$ achieves very large values. For example, for $U^* \sim 3$ the value is close to the peak value observed

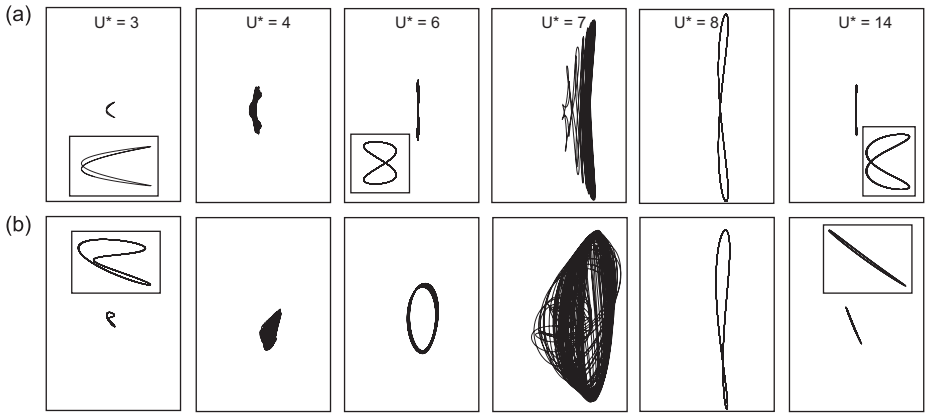

Fig. 3. Comparison of Lissajous figures for the downstream cylinder in (a) tandem and (b) staggered arrangements at various U^*. The figures in the insets show a close-up view of the trajectory.

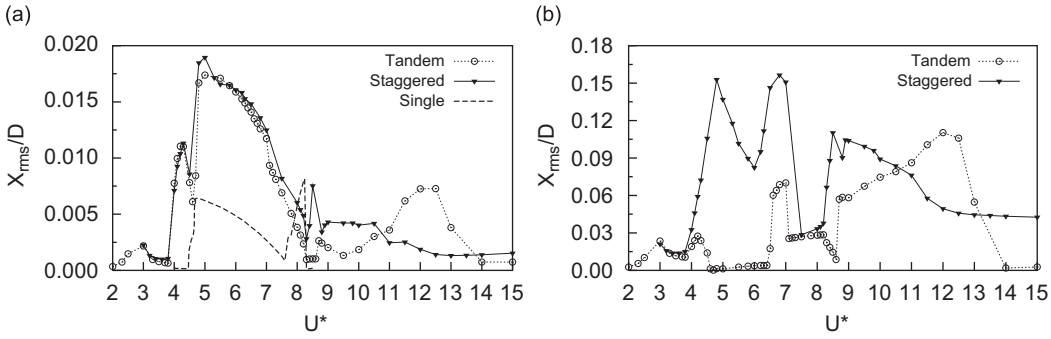

Fig. 4. Variation of the *rms* value of in-line oscillation of (a) upstream cylinder and (b) downstream cylinder in both tandem and staggered arrangements with U^*. The data for a single cylinder is also shown in (a).

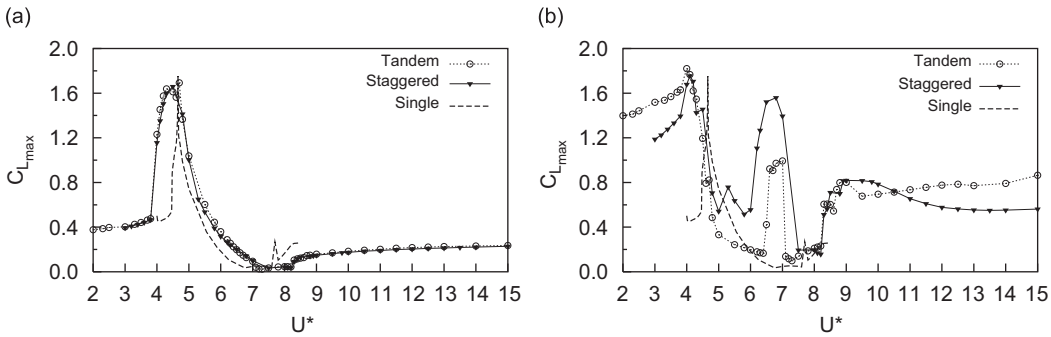

Fig. 5. Variation of the maximum lift coefficient for (a) upstream and (b) downstream cylinder in both tandem and staggered arrangements with U^*. The results for a single cylinder are also shown in the figure.

for the entire U^* range. This is due to the modification in the vortex shedding pattern of the downstream cylinder because of the impingement of vortices shed from the upstream one.

Fig. 6 shows the time histories of lift coefficient and transverse response of the downstream cylinder for $U^* = 6$ and 8. For the tandem arrangement (left column), the mean of both the lift coefficient and transverse oscillation for a cycle is zero. However, this is not the case for the staggered arrangement (right column). The mean is positive at $U^* = 6$ and negative for $U^* = 8$. As will be shown later in the paper, that this is due to the asymmetry of the interaction between the downstream cylinder and vortices released from the upstream cylinder in the staggered arrangement.

5.5. Vortex shedding frequency and synchronization

Fig. 7 shows the variation of nondimensionalized vortex shedding frequency for the two cylinders in tandem and staggered arrangements. The variation of the same quantity for a single cylinder and F_N are also shown. The onset of synchronization/lock-in for cylinders with very low mass ratio corresponds to the U^* where the vortex shedding frequency changes drastically from the value corresponding to that of a stationary cylinder. The lock-in frequency need not be equal to the natural frequency of the system (Williamson and Govardhan, 2004). The synchronization is observed for $4.1 < U^* < 8.3$ for both cylinders. This range is larger than that for a single cylinder.

The change in frequency near the onset of synchronization occurs in two steps. In the first step, the jump occurs to a frequency in-between that of vortex shedding frequency of stationary cylinders and F_N. Lock-in behaviour is observed for a range $4.1 < U^* < 4.8$ after the first jump. In this range, the vortex shedding frequency of the oscillating cylinder is significantly different from F_N. Mittal and Kumar (1999) referred to this phenomenon as soft lock-in. A second jump takes the vortex shedding frequency close to the natural frequency of the system. Both cylinders show lock-in for $U^* \leqslant 8.3$. In the synchronization regime, the two-cylinder system shows larger detuning of the vortex shedding

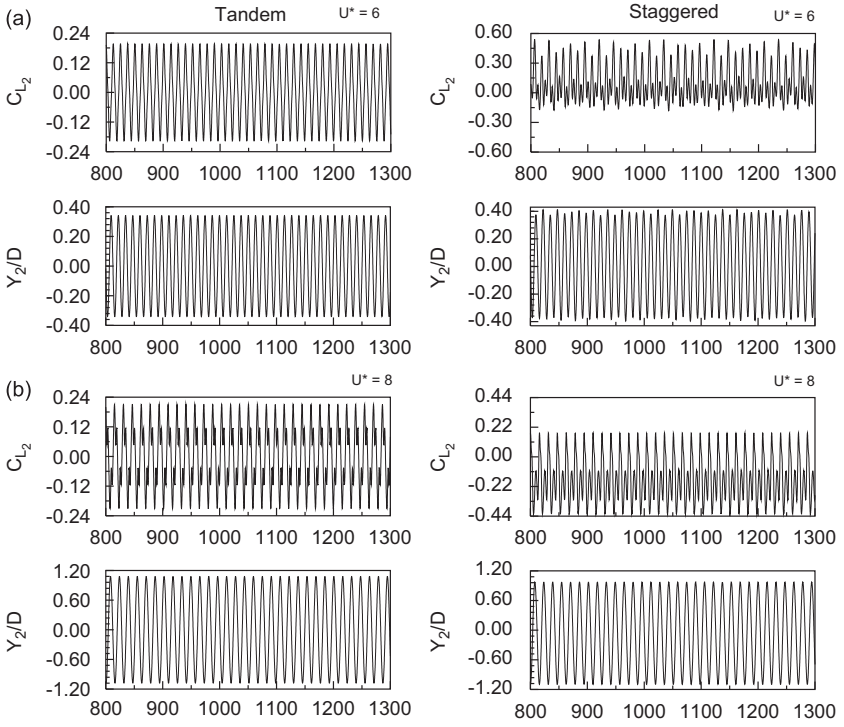

Fig. 6. Time histories of the lift coefficient and transverse response of the downstream cylinder for (a) $U^* = 6$ and (b) $U^* = 8$. The column on the left-hand side is for the two cylinders in tandem while the one on the right-hand side is for staggered arrangement.

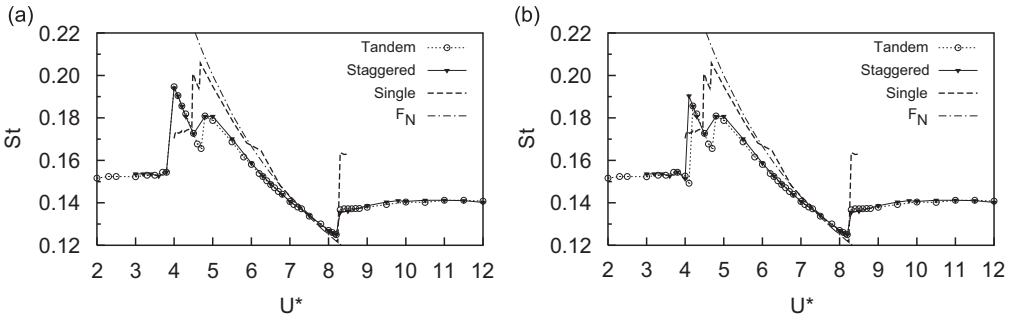

Fig. 7. Variation of the nondimensionalized vortex shedding frequency of (a) upstream cylinder and (b) downstream cylinder in both tandem and staggered arrangements with U^*. The results for a single cylinder are also shown in the figure.

frequency from the natural frequency compared to the single cylinder. The U^* at which the synchronization ends is the same for the single cylinder and the two cylinder arrangements.

An interesting observation from the present computations is that the vortex shedding frequency from the upstream and downstream cylinders are identical in all conditions that are studied. Sumner et al. (2000) also noted a similar behaviour for stationary cylinders in staggered arrangements. They attributed it to the synchronization between the impingement of flow and vortex shedding from the downstream cylinder. The vortex shedding frequency of the two cylinders is identical within and outside the lock-in range. Outside the lock-in range, the vortex shedding frequency is very close to that for stationary cylinders. However, this frequency is quite different than that for a stationary isolated cylinder. For example, at $U^* = 3$ the nondimensionalized vortex shedding frequency is 0.1523 for freely vibrating two cylinders. This is very close to the vortex shedding frequency for two stationary cylinders (= 0.1503). Interestingly, the nondimensionalized vortex shedding frequency for a stationary isolated cylinder is much lower (= 0.128).

5.6. Vortex shedding modes

The flow involving multiple bluff bodies is very complex even when they are stationary. The relative spacing between the bodies plays a crucial role in the fluid dynamic behaviour. The situation can be more complex if one or more bodies are free to oscillate. In the present study, since the downstream cylinder lies in the wake of the upstream one, wake interference occurs. Fig. 8 shows vorticity fields at various U^* for two cylinders in staggered arrangement. The upstream cylinder undergoes regular von Kármán vortex shedding at all U^*, while the downstream cylinder encounters an unsteady inflow. The far wake is very sensitive to U^*. In this work, we focus on the near wake. For the cylinders in tandem arrangement the mean flow remains symmetric with respect to the wake centreline. In this situation, the vortices released from the upper and lower surface of the upstream cylinder experience identical interaction with the downstream cylinder. The stagger in the arrangement of the cylinder leads to asymmetry in the mean wake. Two patterns of vortex shedding are observed in the wake of the downstream cylinder. For $7.1 < U^* < 8.3$ the downstream cylinder experiences a figure of 8 motion and the vortex pattern is similar to that observed in the tandem arrangement. For other values of U^* the cylinder undergoes orbital motion (Fig. 3). In this situation the clockwise vortex, shed from the upstream cylinder, hits the downstream one head on. The counterclockwise vortex from the upstream cylinder only augments the vortex formation at the bottom surface of the downstream cylinder creating a bias in the flow as seen from Fig. 8 at $U^* = 3, 4, 6$ and 14.

5.7. The difference in the vortex interaction in tandem and staggered arrangements

An FFT of the time history of lift force experienced by the downstream cylinder at $U^* = 6$ in the staggered arrangement shows the presence of two frequencies: the most dominant being the vortex shedding frequency (St) and a second equal to twice the first one. A phase difference between the two components at frequencies St and 2St leads to a nonzero mean value as seen in Fig. 6. In order to study this in detail, we look at the time variation of perturbation pressure coefficient, C_p', for a cycle of transverse oscillation of the downstream cylinder. The perturbation pressure is obtained by subtracting the time-averaged pressure from the instantaneous value. The time history of C_p' is shown at two locations on at the upper and lower shoulder on the surface of the cylinder in Fig. 9 (top row). The upper and lower shoulders are also marked as points d and b, respectively. From Fig. 9(a) it is seen that the time variation of C_p' is the same for the upper and lower points of the downstream cylinder when the two cylinders are in tandem arrangement. They are separated by a 180° phase. This reflects that in a lift cycle, the two vortices released from the upstream cylinder go through an identical interaction with the downstream cylinder.

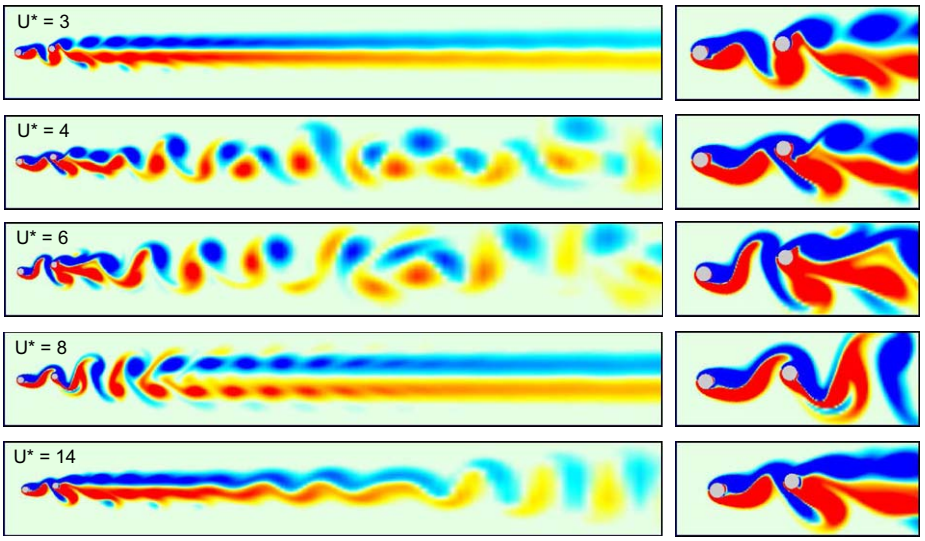

Fig. 8. Instantaneous vorticity fields at various U^* for the fully developed flow past two freely vibrating cylinders in staggered arrangement ($P/D = 5.5D$ and $T/D = 0.7D$). The pictures on the right-hand side show close-up view of the flow near the two cylinders. The blue and red colour denote clockwise and anti-clockwise vorticity, respectively. For interpretation of the reference to colours in the figure legend 8 the reader is referred to web version of this article.

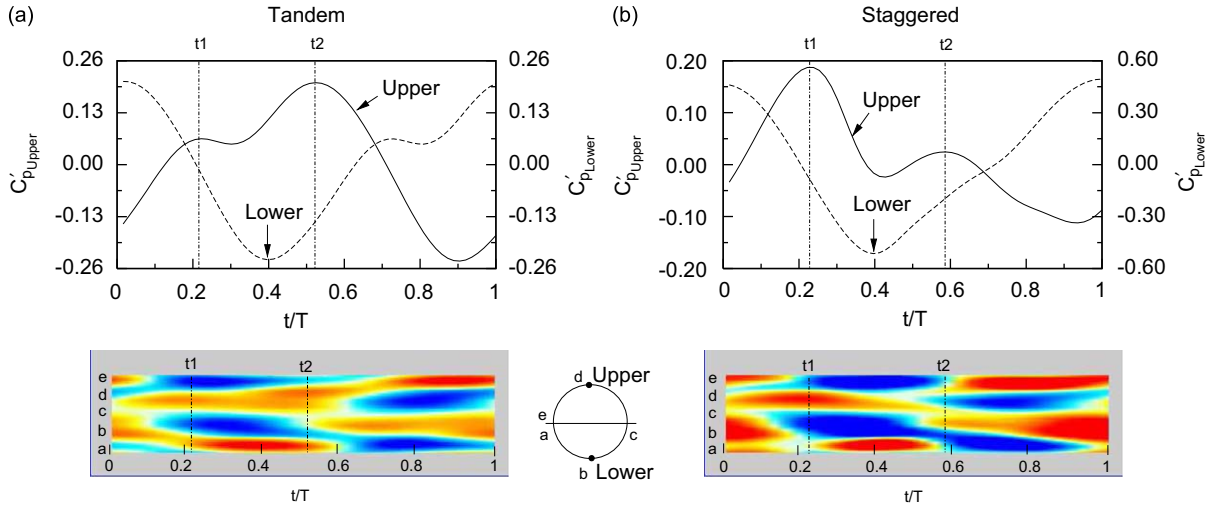

Fig. 9. Time variation of the perturbation pressure coefficient at the upper and lower shoulders of the downstream cylinder in (a) tandem and (b) staggered arrangement for $U^* = 6$ (top row). The variation of the perturbation pressure coefficient along the cylinder surface with time is also shown for a cycle of downstream cylinder oscillation (bottom row).

The variation of C'_p for the downstream cylinder, in the staggered arrangement, is not the same at "Upper" and "Lower" points. This essentially shows that the interaction of the two vortices shed from the upstream cylinder is not the same on both sides of the downstream cylinder. The time variation of C'_p on the lower shoulder of the downstream cylinder is very similar in both tandem and staggered arrangement and is associated with only one major frequency—St. The 2St frequency component is quite weak. However, the 2St frequency is quite significant for the C'_p variation on the upper shoulder. This is further highlighted in the bottom row of Fig. 9 that shows the variation of C'_p along the entire surface of the downstream cylinder with time. It is seen that on the lower surface of the cylinder (a–b–c), the variation of C'_p is very similar in both arrangements. However, the variation at the upper surface of the cylinder (c–d–e) shows differences. For the downstream cylinder in the tandem arrangement, the variation of C'_p shows local peaks at time instants $t1$ and $t2$. The time history of C'_p along the cylinder surface also shows two regions of maximum C'_p corresponding to $t1$ and $t2$. However, the variation of C'_p for the upper surface (c–d–e) of the downstream cylinder in the staggered arrangement shows only one dominant peak. At time $t1$ a clockwise vortex from the upstream cylinder hits the downstream one. This is seen for both arrangements. From the top row of Fig. 9 it is seen that the C'_p on the upper shoulder achieves a maxima at this instant for the staggered arrangement. However, in the tandem arrangement the maximum C'_p on the upper shoulder is achieved at time $t2$ when the vortex formed on the downstream cylinder is about to be released. Another interesting observation from the variation of C'_p for the two arrangements is the phase difference between thevortex formed on the downstream cylinder and the impingement of the vortex on it from the upstream cylinder.

6. Concluding remarks

The vortex-induced vibration of a pair of equal-sized circular cylinders in tandem and staggered arrangements is studied numerically at $\mathrm{Re} = 100$. A stabilized finite element method is utilized to carry out the computations in two dimensions for reduced velocities, $2 \leqslant U^* \leqslant 15$. The cylinders are separated by $5.5D$ in the streamwise direction in both arrangements and are separated by $0.7D$ in the cross-flow direction for the staggered arrangement. In both arrangements, the downstream cylinder lies in the wake of the upstream one and experiences an unsteady in-flow. The response of the cylinders in both tandem and staggered arrangements are compared with each other and with that of a single cylinder. The upstream cylinder in both arrangements behaves qualitatively similarly to an isolated cylinder except that it has slightly larger peak oscillation amplitude. It undergoes large amplitudes of oscillation even at low $U^*(\sim 4)$. This shows that the presence of an equal-sized oscillating cylinder downstream has some effect on the response of the upstream cylinder even though they are well separated.

The downstream cylinder in both arrangements shows very large amplitude of transverse oscillations ($\sim 1.1D$) for a range of U^*. This value of amplitude is same as that observed for free vibrations of an isolated cylinder at higher Re regime. For the downstream cylinder, the peak amplitude of oscillation occurs near the higher U^* end of the synchronization regime. The stagger in the arrangement of cylinders is found to have significant influence in the in-line response of the downstream cylinder, the amplitude of in-line response is larger for the staggered arrangement. The time histories of lift coefficient and transverse oscillation for the downstream cylinder show a nonzero mean value for the staggered arrangement. The mean is zero for the tandem arrangement.

Synchronization/lock-in is observed for a range of U^*. The vortex shedding frequency for the upstream and downstream cylinders is the same in both tandem and staggered arrangements. Both cylinders undergo soft lock-in for a range of U^* which is larger than that observed for a single cylinder. In the synchronization regime, the two-cylinder system shows larger detuning of the vortex shedding frequency from the natural frequency compared to the single cylinder case. Even outside the synchronization regime the vortex shedding frequencies of the two-cylinder arrangements are different from that for a single cylinder.

The cylinders in tandem arrangement undergo a figure of 8 motion similar to that of a single cylinder at all U^*. The upstream cylinder in the staggered arrangement also shows a similar behaviour. However, the downstream cylinder in the staggered arrangement is found to undergo two types of motion: (i) an orbital motion and (ii) figure of 8 motion. During the orbital motion, the dominant frequency in the time variation of both lift and drag experienced by the downstream cylinder is found to be the same. They are also associated with another frequency which is twice that of the dominant one. An analysis of the perturbation pressure coefficient showed that multiple dominant frequencies are due to the modification of the vortex interaction caused by the stagger in the arrangement. The flow shows bias with respect to the wake centreline when the cylinder undergoes orbital motion.

Acknowledgement

Partial support for this work from the Department of Science and Technology, India is gratefully acknowledged.

References

Assi, G.R.S., Meneghini, J.R., Aranha, J.A.P., Bearman, P.W., Casaprima, E., 2006. Experimental investigation of flow-induced vibration interference between two circular cylinders. Journal of Fluids and Structures 22, 819–827.

Bearman, P.W., 1984. Vortex shedding from oscillating bluff bodies. Annual Review of Fluid Mechanics 16, 195–222.

Bokaian, A., Geoola, F., 1984. Wake-induced galloping of two interfering circular cylinders. Journal of Fluid Mechanics 146, 383–415.

Jester, W., Kallinderis, Y., 2004. Numerical study of incompressible flow about transversely oscillating cylinder pairs. ASME Journal of Offshore Mechanics and Arctic Engineering 126, 310–317.

Khalak, A., Williamson, C.H.K., 1999. Motion, forces and mode transitions in vortex-induced vibrations at low mass damping. Journal of Fluids and Structures 13, 813–851.

King, R., Johns, D.J., 1976. Wake interaction experiments with two flexible circular cylinders in flowing water. Journal of Sound and Vibration 45, 259–283.

Laneville, A., Brika, D., 1999. The fluid and mechanical coupling between two circular cylinders in tandem arrangement. Journal of Fluids and Structures 13, 967–986.

Mahir, N., Rockwell, D., 1996. Vortex formation from a forced system of two cylinders, Part 1: tandem arrangement. Journal of Fluids and Structures 10, 473–489.

Mittal, S., Kumar, V., Raghuvanshi, A., 1997. Unsteady incompressible flow past two cylinders in tandem and staggered arrangements. International Journal of Numerical Methods in Fluids 25, 1315–1344.

Mittal, S., Kumar, V., 1999. Finite element study of vortex-induced cross-flow and in-line oscillations of a circular cylinder at low Reynolds numbers. International Journal of Numerical Methods in Fluids 31, 1087–1120.

Mittal, S., Kumar, V., 2001. Flow-induced oscillations of two cylinders in tandem and staggered arrangement. Journal of Fluids and Structures 15, 717–736.

Mittal, S., Kumar, V., 2004. Vortex-induced vibrations of a pair of cylinders at Reynolds number 1000. International Journal of Computational Fluid Dynamics 18, 601–614.

Prasanth, T.K., Behara, S., Singh, S.P., Kumar, R., Mittal, S., 2006. Effect of blockage on vortex-induced vibrations at low Reynolds numbers. Journal of Fluids and Structures 22, 865–876.

Prasanth, T.K., Mittal, S., 2008. Vortex-induced vibrations of a circular cylinder at low Reynolds numbers. Journal of Fluid Mechanics 594, 463–491.

Sarpkaya, T., 2004. A critical review of the intrinsic nature of vortex-induced vibrations. Journal of Fluids and Structures 19, 389–447.

Singh, S.P., Mittal, S., 2005. Vortex-induced oscillations at low Reynolds numbers: hysteresis and vortex shedding modes. Journal of Fluids and Structures 20, 1085–1104.

Sumner, D., Price, S.J., Paidoussis, M.P., 2000. Flow pattern identification for two staggered circular cylinders in cross flow. Journal of Fluid Mechanics 411, 263–303.

Tezduyar, T.E., Behr, M., Liou, J., 1992a. A new strategy for finite element computations involving moving boundaries and interfaces-the deforming-spatial-domain/space-time procedure, I: the concept and the preliminary tests. Computer Methods in Applied Mechanics and Engineering 94 (3), 339–351.

Tezduyar, T.E., Behr, M., Mittal, S., Liou, J., 1992b. A new strategy for finite element computations involving moving boundaries and interfaces- the deforming-spatial-domain/space-time procedure, II: computations of free-surface flows, two liquid flows and flows with drifting cylinders. Computer Methods in Applied Mechanics and Engineering 94 (3), 353–371.

Tezduyar, T.E., Mittal, S., Ray, S.E., Shih, R., 1992c. Incompressible flow computations with stabilized bilinear and linear equal-order-interpolation velocity pressure elements. Computer Methods in Applied Mechanics and Engineering 95, 221–242.

Williamson, C.H.K., Govardhan, R., 2004. Vortex induced vibration. Annual Review of Fluid Mechanics 36, 413–455.

Zdravkovich, M.M., 1977. Review of flow interference between two circular cylinders in various arrangements. ASME Journal of Fluids Engineering 99, 618–633.

Zdravkovich, M.M., 1985. Flow-induced oscillations of two interfering circular cylinders. Journal of Sound and Vibration 101, 511–521.